

A Planar Monopole Antenna with Switchable Dual Band-Notched UWB/Dual-Band WLAN Applications

Mohammad M. Fakharian, Pejman Rezaei, and Vahid Sharbati

Department of Electrical and Computer Engineering
Semnan University, Semnan, 35131-19111, Iran
m_fakharian@semnan.ac.ir, prezaei@semnan.ac.ir, and v.sharbati@semnan.ac.ir

Abstract — In this paper, a planar monopole antenna in ultra-wide band (UWB) frequency range from 2.8 to 10.2 GHz with two notch band of 3.3–4.2 and 4.9–6 GHz is presented. The dual band-notched UWB antenna can be switched to dual wireless local area network (WLAN) frequency bands of 2.2–2.6 and 5–5.9 GHz. The proposed antenna has a simple structure and compact size of 15×15 mm². The antenna in the UWB function uses a circular radiator monopole with an embedded slot in the ground plane. Several stubs are etched on the radiator as rejecting elements. A parasitic element with an ideal switch is used in the backplane to achieve the dual-band WLAN function. In this mode, the stubs in the radiator are as resonating elements. The function of the antenna can be changed by switching states that make the various operating bands. The measurement and simulation results show that the antenna has good characteristics for cognitive radio application where the UWB antenna is required for spectrum sensing and the WLAN band antenna is used for reconfigurable operation.

Index Terms — Dual band-notched, dual-band WLAN, switchable, UWB antenna.

I. INTRODUCTION

One of the methods to develop switchable antennas in cognitive radio (CR) devices is to use the same antenna for both sensing and communication acts. It can be performed by switching ultra-wide band (UWB) sensing antenna to communicate into multiple defined frequency bands [1]. Several designs of UWB antennas with reconfigurability options in frequency agility for CR systems have been implemented so far [2-7].

Recently, frequency switchable antennas that can support the UWB application and wireless local area network (WLAN) bands have been investigated [3, 8-10]. In [3], an incorporated planar UWB/reconfigurable slot antenna is proposed for CR applications. A slot resonator is embedded in the disc monopole radiator to obtain an individual narrowband antenna. A varactor diode is also deliberately inserted across the slot,

providing a reconfigurable frequency function in the range of 5–6 GHz. In [8], an antenna is proposed that is composed of four switches, a rectangular ring slot, a T-shaped stub, a coplanar waveguide feeding line, and two inverted S-shaped slots. By controlling the switches, the antenna is able to provide two operation modes whose operation bands can cover the dual-band WLAN bands and the single band-notched UWB bands. In [9], a rotatable reconfigurable antenna that can support the dual band-notch UWB application and the triple-band WLAN application is presented for CR systems. By controlling the rotational patch at different states, the antenna operates in two WLAN/mobile band and dual band-notched UWB complementary bands. However, these antennas have a complex structure and exhibit some defects in practical applications, require too much antenna space, and their center frequencies are difficult to control.

This paper presents a novel circular monopole antenna with switchable functions for UWB/WLAN applications. Several modified stubs in the radiation patch are used to realize the dual band-notch characteristic for the UWB antenna at worldwide interoperability for microwave access (WiMAX) band (3.3–3.7 GHz), C-band (3.7–4.2 GHz), and WLAN band (5.15–5.825 GHz). By embedding the cleaver-shaped parasitic element in backplane and using a switch between the ground plane and this parasitic element, the antenna is able to provide two operation cases which operation bands can cover the dual-band WLAN (2.4–2.48, 5.15–5.35, 5.725–5.825 GHz) and the dual band-notched UWB bands. Dimensions of the designed antenna are small, and its structure has less complexity and better usefulness. Additionally, novelty in comparison to previously presented antennas is another specification of this design, and with just one switch, two states are investigated.

II. ANTENNA DESIGN AND CONFIGURATION

The proposed monopole antenna fed by a 50-Ohm microstrip line is shown in Fig. 1, which is printed on

an FR4 substrate, with dimensions of $15 \times 15 \times 0.8$ mm³, permittivity 4.4, and loss tangent of 0.02. The antenna consists of a circular radiation patch with four stubs in up and down of it, a ground plane with rectangular-shaped of slot in it, and a cleaver-shaped parasitic element in backplane that contains a rectangular-shaped stub with a thin extruded stub from it. To achieve the desired frequency reconfigurability, one ideal switch is placed between the ground plane and parasitic element. In this study, the ideal switch for reconfigurability is metal bridge, which is achieved based on the proof of concept [9]. The presence of the metal bridge depicts that the switch state is ON; vice versa, the absence of the metal bridge depicts that the switch state is OFF in both simulation and fabrication. The dimension of the ideal switch is selected 0.7×0.2 mm² to be close to the actual dimension of a PIN diode switch. Signal transmission is mainly done by the means of an SMA connector attached to the monopole antenna.

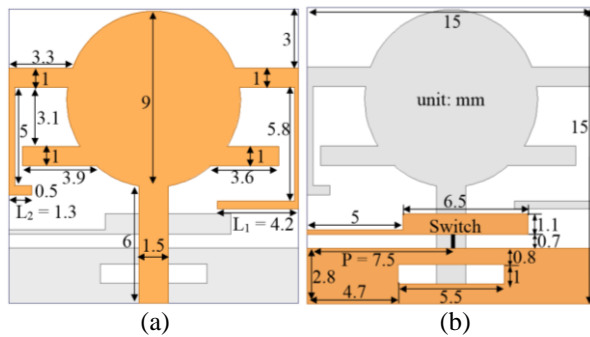


Fig. 1. Geometry of the proposed monopole antenna: (a) front view, and (b) bottom view.

By adjusting the total length of the bent stubs at the top of the patch to a half-wavelength of the rejecting bands, two notched bands with central frequencies of 3.7 and 5.5 GHz for WiMAX/C-band and WLAN can be obtained at UWB function, respectively. Widening bandwidth and operation band in the frequency range of 3.1–10.6 GHz for UWB system can be also achieved by tuning the lower stubs in the radiation patch and inserting a rectangular-shaped slot in the ground plane.

A dual band-notched UWB antenna to the dual-band function at the range of WLAN bands is introduced here by inserting an ideal switch between the ground plane and parasitic element. The position of the switch is determined somehow to create the desired frequency bands. When switch is ON, the proposed monopole antenna operates in dual-band WLAN mode. When switch is OFF, the antenna operates in dual band-notched UWB mode. When the proposed antenna works in dual-band WLAN mode, the two bent stubs at the top of the radiation patch provide the electrical current paths for producing the 2.4 and

5.5 GHz resonant frequency bands. The performance of the antenna is optimized and simulated with the Ansoft HFSS [11]. For this purpose, a wide parametric study is performed, and the final dimensions of the antenna are specified, as shown in Fig. 1. In addition, some important parameters of the proposed monopole antenna will be discussed in Section III in detail.

III. RESULTS AND DISCUSSION

A. Dual band-notched UWB antenna design

Figure 2 shows the schematic of the designed antenna in five steps used for dual band-notched UWB performance simulation studies. Comparisons among input reflection coefficients ($|S_{11}|$) for an ordinary circular monopole antenna [step 1], inserting a rectangular-shaped slot in the ground plane [step 2], attaching two rectangular-shaped stubs in the down of radiating patch [step 3], attaching a bent stub at the top of the radiating patch in the right [step 4], and the proposed antenna [step 5] are also respectively considered in Fig. 2. As shown in Fig. 2, the monopole antenna with slotted ground plane has wider impedance matching in comparison to the same antenna without slot in the ground plane. The current distribution on the slotted ground plane affects the impedance matching and the upper frequency bandwidth of the antenna. Also, it is found that by adding the stubs in the down of the radiating patch, the antenna can cover the full UWB band from 2.8–10.8 GHz. The first notched frequency (3.3–4.2 GHz) is achieved by the bent-shaped stub in the top right of the radiating patch, and eventually by using another bent-shaped stub in the top left of the radiating patch, a dual band-notch function is obtained that covers all the 5.2/5.8 GHz WLAN, 3.5/5.5 GHz WiMAX, and 4 GHz C-bands.

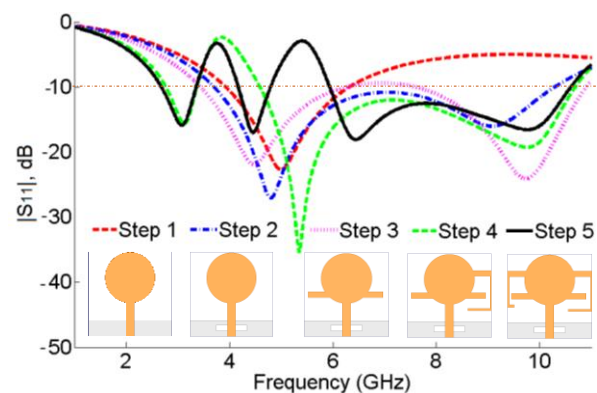


Fig. 2. Simulated $|S_{11}|$ of final design of the dual band-notched UWB antenna in five steps.

In order to understand the phenomenon behind the dual band-notch UWB performance, the simulated current distributions on the radiating patch at the

notched frequencies of 3.8 and 5.5 GHz are shown in Figs. 3 (a) and 3 (b), respectively. It can be observed in these figures that the current is concentrated at the edges of the U-shaped stub and the L-shaped stub and oppositely directed between the interior and exterior edges at 3.8 and 5.5 GHz, respectively. Therefore, the resultant radiation fields can be cancelled out, and high attenuation near the resonant frequency is achieved, thus the resulting notched band. By adjusting the dimensions of the U- and L-shaped stubs, the center frequencies of the lower and higher notched band can be independently controlled.

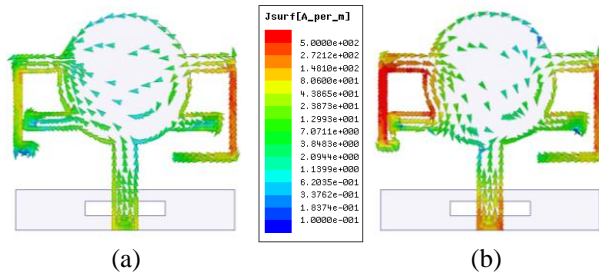


Fig. 3. Simulated current distributions of the dual band-notched UWB antenna at the notch frequencies of: (a) 3.8 GHz and (b) 5.5 GHz.

Figure 4 shows the simulated $|S_{11}|$ of the dual band-notched UWB antenna for different dimensions of U- and L-shaped stubs. Figure 4 (a) presents the simulated $|S_{11}|$ curves of the antenna with the length $L_1 = 3.2, 4.2,$ and 5.2 mm. It is found that with the increase of the length, the central frequency of the first notched band moves to a lower frequency, whereas the second notched band is slightly affected. Second, Fig. 4 (b) shows how the length of the L_2 affects the antenna performance. When the length of L_2 changes from 0.3 to 2.3 mm, the second notched band moves to the lower frequency, whereas the first notched band is not affected. As a result, we can adjust independently the notch frequencies by varying the length of L_1 and L_2 .

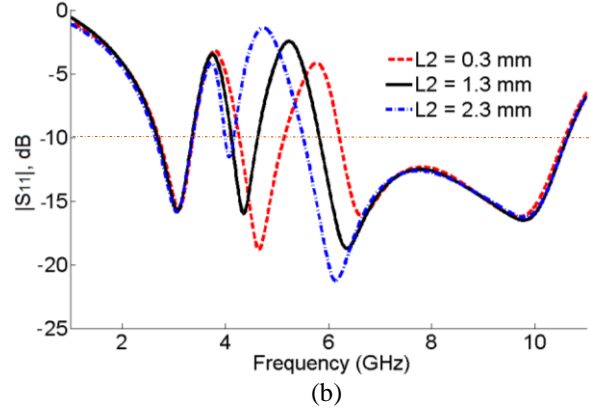
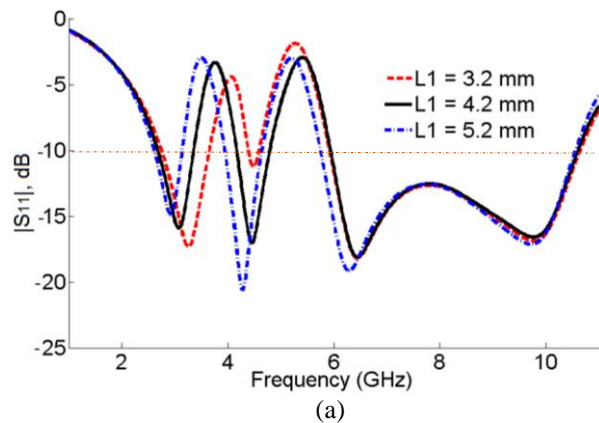


Fig. 4. Simulated $|S_{11}|$ of the dual band-notched UWB antenna with different values of: (a) L_1 and (b) L_2 .

B. Switchable dual band-notched UWB/dual-band WLAN antenna design

The dual band-notched UWB antenna that was introduced in the Section A can be applied as a dual-band WLAN antenna using a parasitic element in the backplane and inserting a metal strip as ideal switch between the ground plane and it. Figure 5 shows the structure of the various antennas in three steps used for the dual-band performance simulation studies from the dual band-notched UWB antenna. $|S_{11}|$ for dual band-notched UWB antenna [step 1], with placing a cleaver-shaped parasitic element in the antenna backplane [step 2], and final design by placing a metal strip between parasitic element and ground planer [step 3] are also compared in Fig. 5. As shown in Fig. 5, the frequency bandwidth of the UWB antenna is not much affected by using the parasitic element in the steps 1 and 2, and the upper frequency just declined from 10.8 to 10.2 GHz. However, it is found that by inserting the metal strip, a dual-band function is achieved that covers all the $2.4/5.2/5.8$ GHz WLAN bands. Therefore, the phenomenon of switching between the dual band-notched UWB and the dual-band WLAN performances is clarified here by the absence/presence of the metal strip for OFF/ON states in the steps 2/3, respectively.

To understand the operation theory of the antenna at the dual band-notch UWB with OFF switch and dual-band WLAN with ON switch, the current distributions of the two cases are shown in Fig. 6. As shown in Figs. 6 (a) and 6 (b), current flows are more dominant on the transmission line and are dispersed by the means of the stubs and concentrated around two sides of the rectangular slot in the ground plane in both frequency of 4.5 and 9.5 GHz. Also in Figs. 6 (a) and 6 (b), current flows on the feed line and the lower part of the patch have similar directions. In these structures, the central and top parts of the patch have current flows in rotational directions and electrically are neutralized. As

shown in Figs. 6 (a) and 6 (b), the current concentrated on the edges of the interior and exterior of the parasitic element in backplane at these frequencies. This figure shows that the electrical current does not change direction along the top edge of the ground plane. Therefore, the radiating power and bandwidth will not decrease significantly.

When the antenna works in the dual-band WLAN mode, the switch between the parasitic element and ground plane is ON. The parasitic element couples to the ground plane. In this case, for the 2.4 GHz excitation, clearly a larger surface current distribution is observed to flow along not only the feeding line, but also the stubs, especially the right side stub, as shown in Fig. 6 (c). This indicates that this stub does effectively provide the electrical current path for producing the 2.4 GHz resonant frequency band. However, for the 5.5 GHz excitation, the surface currents mainly flow along the left side stub, as shown in Fig. 6 (c). The difference between the two current distributions is because the proposed design can generate two various frequency bands that meet the demand of the dual-band WLAN application. The dual-band antenna has a slightly higher efficiency rather than dual band-notch UWB antenna in the 2.4 GHz radiating band, which is mainly owing to the electromagnetic coupling and the new resonant properties from the parasitic element which connected to the ground plane.

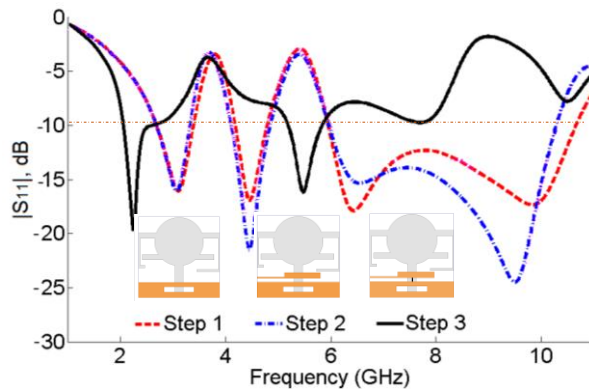


Fig. 5. Simulated $|S_{11}|$ of final design of the dual-band WLAN antenna in four steps.

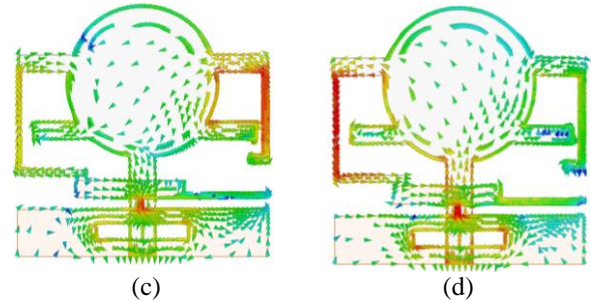
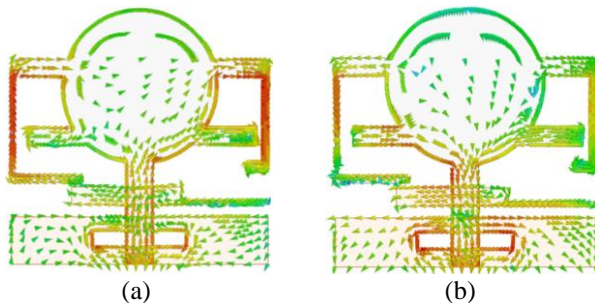


Fig. 6. Simulated current distributions of the antenna in the two cases; dual band-notch UWB mode at: (a) 4.5 GHz, (b) 9.5 GHz, and the dual-band WLAN mode at (c) 2.4 GHz, (d) 5.5 GHz.

To further investigate the design of the dual-band WLAN antenna, the influence of the position of the switch on the $|S_{11}|$ curves with various values of P is shown in Fig. 7. The position of switch is important in order to create desirable frequency bands in the WLAN mode. As shown in Fig. 7, the center frequencies of the lower and higher bands decrease with the decrease of P . Moreover, the bandwidth and impedance matching of the upper band can be controllable by changing the position of the switch.

To evaluate the performance of the proposed switchable antenna, the antennas with both switches ON/OFF are fabricated and measured. The prototype of the fabricated antenna is also shown in Fig. 8 (a). The simulated and measured $|S_{11}|$ of the switchable antenna with switch OFF/ON in the UWB/WLAN modes are shown in Fig. 8 (b). The discrepancy in the $|S_{11}|$ between the simulated and the measured may be mostly attributed to the effects of the SMA port, soldering, and manufacturing tolerance. In the dual-band WLAN mode, the switch is ON and the measured lower band for lower than -10 dB is from 2.2 to 2.6 GHz, and the measured higher band covers from 5 to 5.9 GHz. In the dual band-notch UWB mode, the switch is OFF and the antenna has a wideband performance of 2.8 to 10.2 GHz, covering the UWB frequency band with dual notched bands of 3.3–4.2 and 4.9–6 GHz for greater than -10 dB. Thereby, we can control the switches ON and OFF to allow the proposed antenna to work in underlay and overlay modes for CR communications. The proposed antennas can also be used for multimode wireless communication systems by controlling the switches at ON and OFF states.

The measured peak gain of the antenna versus frequency at the broadside direction is shown in Fig. 9. The antenna gain in the dual-band WLAN mode is more than 2.2 dB over the operating bands. Figure 9 also indicates that the gain of the dual band-notch UWB antenna is between 0–8 dB and has a comprehensive level during frequency bands except for two notched

bands at 3.8 and 5.5 GHz. The gains drop to -6.2 dB at lower notch band and -3.9 dB at the higher notch band.

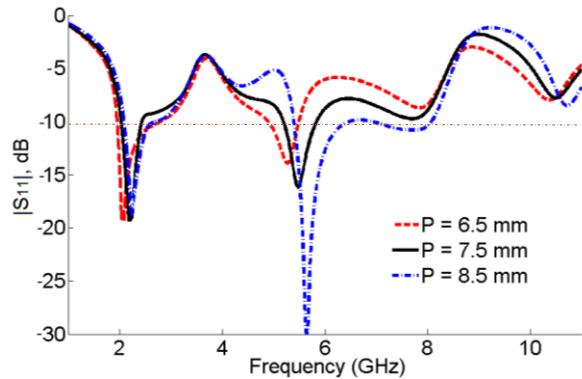


Fig. 7. Simulated $|S_{11}|$ of the dual-band WLAN antenna with different values of P .

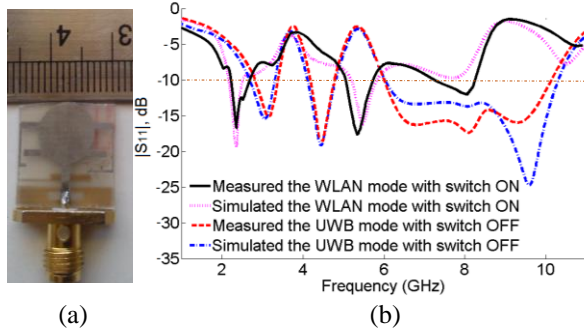


Fig. 8. (a) Prototypes of the antennas in top view. (b) $|S_{11}|$ of the antennas in the UWB/WLAN modes.

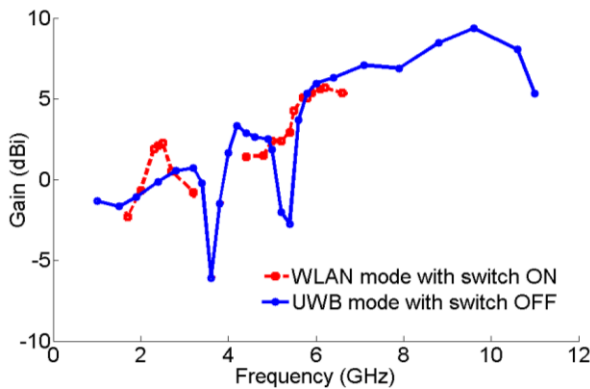


Fig. 9. Measured peak gain of the antenna in the UWB/WLAN modes.

The measured radiation patterns of two fabricated antennas in the two modes with switch ON/OFF are shown in Fig. 10. The antenna with switch ON/OFF can provide a nearly omnidirectional characteristic in H-plane and a dipole-like radiation characteristic in E-

plane. Furthermore, the broadside directions of the two modes are almost identical. The rotation between low-frequency and high-frequency patterns results in the UWB mode is mostly due to the small ground plane effects and the change of excited surface current distributions on the system ground plane at high frequencies.

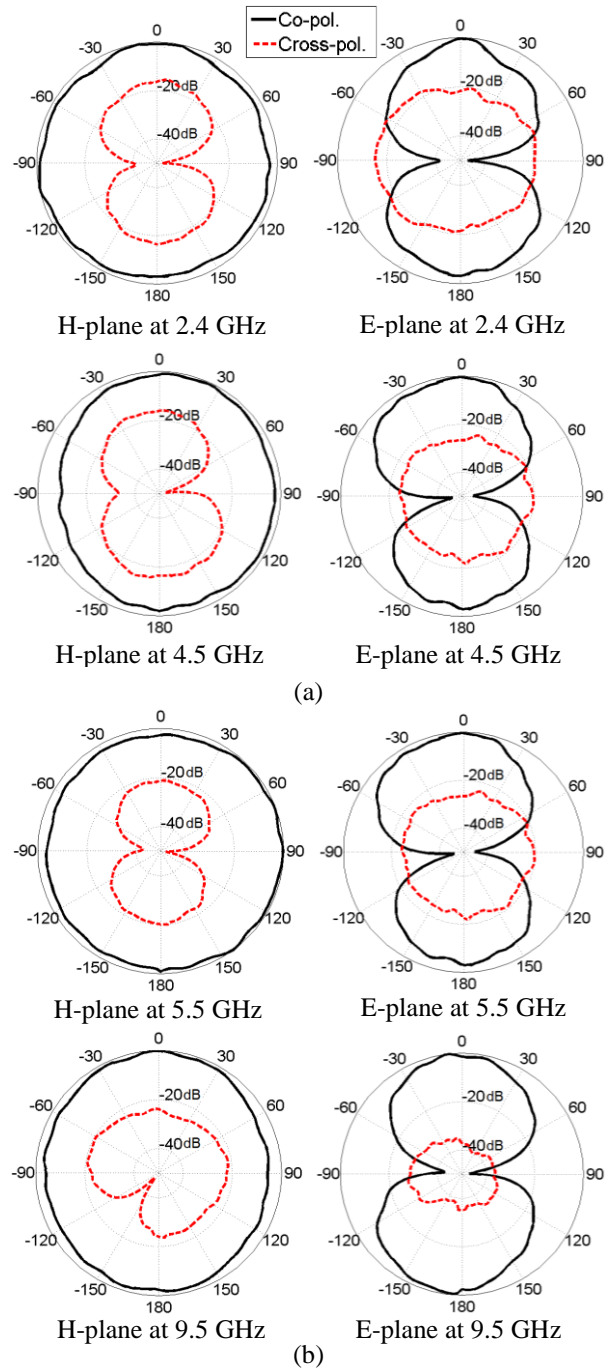


Fig. 10. Measured radiation patterns of the antenna in the two modes: (a) dual-band WLAN mode and (b) dual band-notched UWB mode.

IV. CONCLUSION

A planar monopole antenna with switchable frequency bands for dual band-notched UWB/dual-band WLAN applications has been introduced. It has been shown that using a rectangular slot in the ground plane with four stubs etched on the circular radiator patch can enhance bandwidth from 2.8 to 10.9 GHz with dual stop bands, which are exempt from interfaces with existing WiMAX band, C-band, and WLAN system. In addition, using a rectangular parasitic element in backplane and embedding an ideal switch in proper situations between the parasitic element and ground plane, the antenna can operate in two modes, namely, the dual band-notched UWB mode and the dual-band WLAN frequency mode. This antenna can offer sensing and communicating functions with a small size by controlling ideal switch that is either in the ON or the OFF position. The $|S_{11}|$ of the antenna was measured and agreed well with the simulation results. The measured radiation patterns and gain have been also demonstrated for different operating states of the antenna. The antenna is intended for use in multi radio wireless applications and future CR communications.

ACKNOWLEDGMENT

This work has been supported financially by the Office of Brilliant Talents at the Semnan University. The authors would like to thank all the members of the Antenna Laboratory at Iran Telecommunication Research Center (ITRC), especially Mr. Solat and Mr. Mirabdollahi, for their cooperation.

REFERENCES

- [1] T. Aboufoul, A. Alomainy, and C. Parini, "Reconfiguring UWB monopole antenna for cognitive radio applications using GaAs FET switches," *IEEE Antennas Wireless Propag. Lett.*, vol. 11, pp. 392-394, 2012.
- [2] M. M. Fakharian and P. Rezaei, "Very compact palmate leaf-shaped CPW-fed monopole antenna for UWB applications," *Microw. Optic. Tech. Lett.*, vol. 56, no. 7, pp. 1612-1616, 2014.
- [3] E. Erfani, J. Nourinia, Ch. Ghobadi, M. Niroo-Jazi, and T. A. Denidni, "Design and implementation of an integrated UWB/reconfigurable-slot antenna for cognitive radio applications" *IEEE Antennas Wireless Propag. Lett.*, vol. 11, pp. 77-80, 2012.
- [4] M. M. Fakharian, P. Rezaei, and A. A. Orouji, "A novel slot antenna with reconfigurable meander-slot DGS for cognitive radio applications," *Appl. Comput. Electromagn. Soc. J.*, vol. 30, no. 7, pp. 748-753, 2015.
- [5] T. Wu, R. L. Li, S. Y. Eom, and S. S. Myoung, "Switchable quad-band antennas for cognitive radio base station applications," *IEEE Trans. Antennas Propag.*, vol. 58, no. 5, pp. 1468-1476,

2010.

- [6] Y. Li, W. Li, and W. Yu, "A compact reconfigurable antenna using SIRs and switches for ultra wideband and multi-band wireless communication applications," *Appl. Comput. Electromagn. Soc. J.*, vol. 28, no. 5, pp. 427-440, 2013.
- [7] M. M. Fakharian, P. Rezaei, and A. A. Orouji, "Reconfigurable multiband extended U-slot antenna with switchable polarization for wireless applications," *IEEE Antennas Propag. Mag.*, vol. 57, no. 2, pp. 194-202, 2015.
- [8] P. Lotfi, M. Azarmanesh, and S. Soltani, "Rotatable dual band-notched UWB/triple-band WLAN reconfigurable antenna," *IEEE Antennas Wireless Propag. Lett.*, vol. 12, pp. 104-107, 2013.
- [9] B. Li, J. Hong, and B. Wang, "Switched band-notched UWB/dual-band WLAN slot antenna with inverted S-shaped slots," *IEEE Antennas Wireless Propag. Lett.*, vol. 11, pp. 572-575, 2012.
- [10] G. Zhang, J. S. Hong, B. Z. Wang, and G. Song, "Switched band-notched UWB/WLAN monopole antenna," *Appl. Comput. Electromagn. Soc. J.*, vol. 27, no. 3, 2012.
- [11] Ansoft High Frequency Structure Simulator (HFSS), ver. 11, Ansoft Corp., Framingham, MA, 2010.



Mohammad M. Fakharian was born in Tehran, Iran, in 1987. He received the B.S. and M.S. degrees in Electrical Engineering from Semnan University, Semnan, Iran, in 2009 and 2012, respectively. Currently, he is working towards the Ph.D. degree in Communication Engineering from the Semnan University.

His research interests include low-profile antennas for wireless communication, reconfigurable antennas, and electromagnetic theory: numerical methods and optimization techniques.



Pejman Rezaei was born in Tehran, Iran, in 1977. He received the B.S. degree in Electrical-Communication Engineering from Communication Faculty, Tehran, Iran, in 2000, and the M.S. and Ph.D. degrees from Tarbiat Modarres University, Tehran, Iran,

in 2002 and 2007, respectively. Currently, he is Assistant Professor in the Semnan University, Semnan, Iran.

His current research interests are Electromagnetics theory, theory and design of antenna, metamaterial structure, and satellite communication.



Vahid Sharbati was born in Gorgan, Iran, in 1986. He received the B.S. degree in Electrical Engineering from Mazandaran University, Sari, Iran, in 2009. Currently, he is working towards the M.S. degree in Communication Engineering from the Semnan University. His current interest is in reconfigurable microstrip antennas.